

Probing the DNA-binding behavior of tryptophan incorporating mixed-ligand complexes

Natarajan Raman · Sivasangu Sobha ·
Muthusamy Selvaganapathy

Received: 1 November 2011 / Accepted: 6 January 2012
© Springer-Verlag 2012

Abstract Mixed-ligand Cu(II), Ni(II), Co(II), and Zn(II) complexes using a tryptophan-derived Schiff base (obtained by the condensation of tryptophan and benzaldehyde) as the primary ligand and 1,10-phenanthroline as the co-ligand were synthesized and characterized analytically and spectroscopically by performing elemental analyses, magnetic susceptibility and molar conductance measurements, UV-Vis, IR, NMR, and FAB-MS. The binding properties of metal complexes with DNA were investigated by electronic absorption spectroscopy, cyclic voltammetry, and by performing viscosity measurements, and the results showed that these complexes have the ability to interact with DNA via an intercalative mode. The DNA cleavage efficiencies of these complexes with pUC19 DNA were investigated by gel electrophoresis. The complexes were found to promote the cleavage of pUC19 DNA from the supercoiled form I to the open circular form II and the linear form III in the presence of ascorbic acid. Finally, the in vitro antibacterial activities of the Schiff base and its mixed-ligand metal complexes were screened against the bacteria *Staphylococcus aureus*, *Bacillus subtilis*, *Pseudomonas aeruginosa*, *Escherichia coli*, and *Salmonella typhi*. The antibacterial screening data revealed that the complexes show growth inhibitory activity against bacteria.

Keywords Tryptophan-derived Schiff base · Mixed-ligand complexes · DNA binding · DNA cleavage · Antibacterial activity

Introduction

The medicinal uses and applications of metals and metal complexes are of increasing clinical and commercial importance. Recent advances in chelation research have paved the way for the development of “magic bullets” for chemotherapy using different strategies and pharmacological manipulation, thus demonstrating the significant potential of the utilization of metal complexes as drugs, and highlighting that medical inorganic biochemistry is a flourishing field [1]. Physiologically interesting mixed-ligand complexes of amino acids with heavy metal ions play an important role in biological systems, and have proven to be a subject of great interest to researchers [2–8]. Complexes of amino acids are involved in the exchange and transport of trace metal ions in the human body [9].

Binding studies of small molecules to DNA are very important in the development of DNA molecular probes and new therapeutic reagents. Over the past few decades, DNA-binding metal complexes have been extensively studied as DNA structural probes, DNA-dependent electron transfer probes, DNA footprinting and sequence-specific cleaving agents, and potential anticancer drugs [10–13]. Many compounds exert their antitumor activity by binding to DNA, and can damage DNA in cancer cells, blocking the division of cancer cells and causing cell death [14].

The interaction of metal complexes with DNA is an area of intense interest to both inorganic chemists and biochemists. Transition metal complexes have been widely exploited in probes of nucleic acid structure, and they show nuclease activity. The important criterion for the development of metallodrugs as chemotherapeutic agents is the ability of the metallodrug to cause DNA cleavage [15].

Bacterial resistance is a major global health problem, along with multidrug resistance in pathogenic species.

N. Raman (✉) · S. Sobha · M. Selvaganapathy
Research Department of Chemistry, VHNSN College,
Virudhunagar 626 001, India
e-mail: drn_raman@yahoo.co.in

There is an urgent need to develop new antibacterials with novel mechanisms of action to overcome the problem of resistance [16]. Therefore, researchers are increasingly turning their attention to folk medicine, looking for new leads to develop better drugs for treating microbial infections.

Bearing these facts in mind, in this paper we describe the synthesis, structures, and antibacterial and cleavage studies of a tryptophan-derived Schiff base and its mixed-ligand transition metal complexes. To the best of our knowledge, this is the first report on the chemical nuclease activity of Schiff base mixed-ligand metal complexes of tryptophan derivatives containing 1,10-phenanthroline and various metal ions. The electron-transfer mechanism of the mixed-ligand metal complexes was investigated using cyclic voltammetry. The results enhance our understanding of novel agents for targeting nucleic acids, as well as aid in the synthesis of novel antibacterial drugs for bacterial infections.

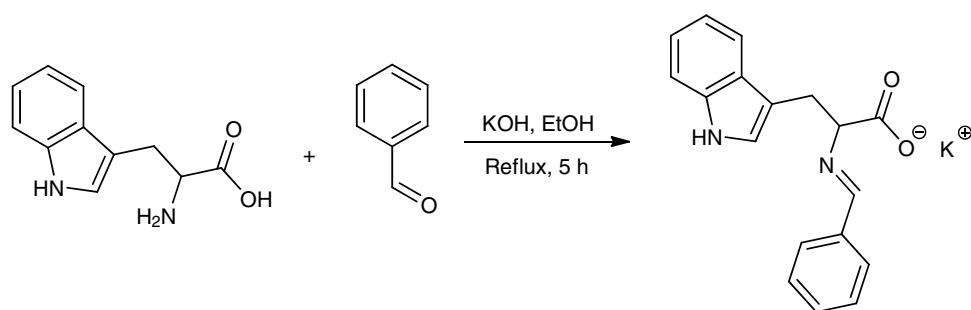
Results and discussion

The Schiff base ligand and its Cu(II), Ni(II), Co(II), and Zn(II) mixed-ligand complexes were synthesized and characterized based on spectral and elemental analysis data. The complexes were found to be air stable. The ligand was soluble in common organic solvents, and all of its complexes were freely soluble in CHCl_3 , DMF, and DMSO. The preparation of the Schiff base is presented schematically in Fig. 1.

Elemental analysis and molar conductivity measurements

Elemental analyses of the Schiff base ligand (KL, **1**) and its complexes were in agreement with the assigned formulae. The metal complexes were dissolved in DMSO and the molar conductivities of 10^{-3} mol/dm³ solutions were measured at 25 °C. The high molar conductance values ($45.37\text{--}58.75 \Omega^{-1} \text{cm}^2 \text{mol}^{-1}$) of the complexes support their electrolytic nature.

Fig. 1 Synthesis of the Schiff base ligand **1**



UV spectra measurements

The geometries of the metal complexes were deduced from the electronic spectra and magnetic data for the complexes. The electronic spectra for the complexes were recorded in DMSO solution. All of the complexes show a high-energy absorption band in the region $27,248\text{--}33,112 \text{ cm}^{-1}$. This transition can be attributed to a charge-transfer band. The electronic spectrum of the copper(II) complex **2** displays a $d\text{--}d$ transition band in the region $13,586 \text{ cm}^{-1}$, which is due to the ${}^2E_g \rightarrow {}^2T_{2g}$ transition. This $d\text{--}d$ transition band strongly favors a distorted octahedral geometry around the metal ion. The absorption spectrum of the nickel(II) complex **3** displays three $d\text{--}d$ bands at $14,749$, $17,168$, and $23,392 \text{ cm}^{-1}$. These bands correspond to ${}^3A_{2g}(\text{F}) \rightarrow {}^3T_{2g}(\text{F})$ (ν_1), ${}^3A_{2g}(\text{F}) \rightarrow {}^3T_{1g}(\text{F})$ (ν_2), and ${}^3A_{2g}(\text{F}) \rightarrow {}^3T_{1g}(\text{P})$ (ν_3) transitions, which are characteristic of an octahedral geometry. This geometry is further supported by its magnetic susceptibility value (3.21 BM). The electronic spectrum of the cobalt(II) complex **4** displays three $d\text{--}d$ transition bands in the regions $14,992$, $17,513$, and $22,652 \text{ cm}^{-1}$, which can be assigned to ${}^4T_{1g}(\text{F}) \rightarrow {}^4T_{2g}(\text{F})$ (ν_1), ${}^4T_{1g}(\text{F}) \rightarrow {}^4A_{2g}(\text{F})$ (ν_2), and ${}^4T_{1g}(\text{F}) \rightarrow {}^4T_{2g}(\text{P})$ (ν_3) transitions. This indicates that the complex of Co(II) is a six-coordinate complex, and probably has an octahedral geometry, which is also supported by its magnetic susceptibility value (4.88 BM). The Zn(II) complex **5** is diamagnetic. According to the empirical formula, an octahedral geometry is proposed for this complex.

Mass spectra

The mass spectrum of the Schiff base ligand showed a peak at $m/z = 330$ corresponding to the $[\text{C}_{18}\text{H}_{15}\text{KN}_2\text{O}_2]$ ion. The spectrum also exhibited peaks for the fragments at $m/z = 238$, 115 , 90 , and 77 , corresponding to $[\text{C}_{11}\text{H}_7\text{KN}_2\text{O}_2]$, $[\text{C}_8\text{H}_5\text{N}]$, $[\text{C}_7\text{H}_6]$, and $[\text{C}_6\text{H}_5]$. The spectra of the Cu(II), Co(II), Ni(II), and Zn(II) complexes showed molecular ion peaks at $m/z = 715$ (M^+), 711 (M^+), 710 (M^+), and 717 ($[\text{M}+1]^+$), respectively. The Cu(II) complex gave a fragment ion peak with the loss of one fragment of phenanthroline at $m/z = 534$. All these fragments lead to

the formation of the species [ML], which further undergoes demetallation to yield the species [L], which gives the fragment ion peak at $m/z = 291$.

IR spectra

The modes and sites of the coordination of the ligand to the metal ions were investigated by comparing the infrared spectra of the free ligand with those of its metal complexes. The IR spectra of the complexes were very similar to each other, except for some slight shifts and changes in intensity by a few vibration bands with different metal ions, which indicate that the complexes have similar structures. The characteristic $\nu(\text{NH})$ mode due to the NH group of the tryptophan moiety present in the Schiff base ligand was observed at $3,252\text{ cm}^{-1}$. The appearance of this band in all of the complexes indicates that the NH group is free from complexation. In the IR spectrum of the Schiff base ligand, the band observed at $1,614\text{ cm}^{-1}$ was shifted to a lower frequency by $10\text{--}33\text{ cm}^{-1}$ on complexation, suggesting the coordination of the azomethine nitrogen [17]. Moreover, the coordination of the ligand to the metal center via the carboxylic group is quite apparent based on the difference in the positions of the maxima observed for $\nu_{\text{sy}}(\text{COO}^-)$ and $\nu_{\text{asy}}(\text{COO}^-)$. The bands were detected at $1,375$ and $1,456\text{ cm}^{-1}$ for the free ligand, so $\Delta\bar{\nu} = 81\text{ cm}^{-1}$. For comparison, $\nu_{\text{sy}}(\text{COO}^-)$ and $\nu_{\text{asy}}(\text{COO}^-)$ were recorded at $1,315\text{--}1,319$ and $1,444\text{--}1,427\text{ cm}^{-1}$, respectively, for all of the metal complexes. These results reveal that the organic ligand is involved in coordination through the carboxyl group. The new bands in the region of $503\text{--}516$ and $470\text{--}484\text{ cm}^{-1}$ in the spectra of the complexes can be assigned to the stretching frequencies of (M–O) and (M–N) bonds, respectively.

Nuclear magnetic resonance spectra

The ^1H NMR spectra of the Schiff base and its zinc(II) complex were recorded at room temperature in CDCl_3 . The signal at $\delta = 10.30$ ppm (s, 1H) in the spectrum for the Schiff base, assigned to the $-\text{NH}$ proton of tryptophan, remained unchanged in the zinc(II) complex. This shows that the $-\text{NH}$ group does not take part in complexation. The ligand also showed one singlet at 8.90 ppm due to the azomethine (CH=N) proton, and a multiplet signal at around $6.81\text{--}7.39$ ppm due to indole protons of the tryptophan moiety. Moreover, it showed a phenyl multiplet signal at $7.49\text{--}7.77$ ppm due to aromatic protons of the benzaldehyde moiety present in the tryptophan-derived Schiff base. In the ^1H NMR spectrum of the Zn(II) complex **5**, the protons of the Schiff base ligand were shifted downfield due to the coordination with the metal ion. Further, a set of multiplets was observed in the range

$7.01\text{--}7.43$ ppm due to the presence of aromatic protons. The resonance peaks observed in the spectrum of the $[\text{ZnL}(\text{phen})_2]\text{Cl}$ complex at $\delta = 7.77\text{--}8.26$ ppm were assigned to the protons of 1,10-phenanthroline (phen). The zinc(II) complex also showed a multiplet signal at $6.63\text{--}6.94$ ppm due to indole protons present in the Schiff base ligand. The azomethine proton ($-\text{CH}=\text{N}$) signal in the spectrum of the zinc complex was shifted downfield compared to the free ligand, suggesting deshielding of the azomethine group due to coordination with the metal ion. The ^{13}C NMR spectrum of the ligand showed aromatic carbons at $105.62\text{--}117.95$ ppm and indole carbons at $118.74\text{--}136.62$ ppm. The ligand also showed the COO^- carbon at 171.56 ppm and the $\text{HC}=\text{N}$ carbon at 167.11 ppm, which were shifted downfield (to 165.47 and 157.25 ppm, respectively) upon coordination, indicating that the COO^- and $\text{HC}=\text{N}$ groups participate in complex formation. There were no appreciable changes in other peaks.

Electron paramagnetic resonance spectra

The EPR spectrum of the copper complex **2** provides important information relating to the metal ion environment. EPR spectra were recorded in DMSO at liquid nitrogen temperature (LNT) and at room temperature (RT). The spectrum of the copper complex at RT showed one intense absorption band at high field, and is isotropic due to the tumbling motion of the molecules. However, at LNT, this complex showed well-resolved peaks in the low-field region. The copper complex had $A_{\parallel} = 156.4 > A_{\perp} = 34.1$; $g_{\parallel} = 2.259 > g_{\perp} = 2.066$, which suggests that the complex is present in an axially elongated octahedral geometry, and that the unpaired electron lies predominantly in the $d_{x^2-y^2}$ orbital. The axial symmetry parameter G is defined as

$$G = \frac{g_{\parallel} - 2.0023}{g_{\perp} - 2.0023}$$

If $G > 4.0$, the local tetragonal axes are aligned parallel to each other, or are only slightly misaligned. If $G < 4.0$, significant exchange coupling is present and the misalignment is appreciable. The observed value for the exchange interaction parameter for the copper complex ($G = 4.04$) suggested that the local tetragonal axes are aligned parallel to each other or are slightly misaligned, and the unpaired electron is present in the $d_{x^2-y^2}$ orbital. This result also indicates that exchange coupling effects do not operate in the present complex [18]. Based on the above spectral and analytical data, the proposed geometry of the metal(II) complexes is shown in Fig. 2.

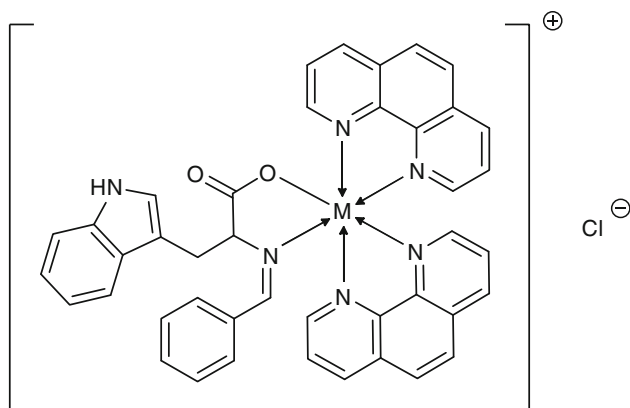


Fig. 2 The proposed structure of the metal complexes. M = Cu(II), Ni(II), Co(II), or Zn(II)

Investigating the interactions of the metal complexes with DNA using electronic absorption spectroscopy

Electronic absorption spectroscopy has proven to be one of the most useful techniques applied in DNA-binding studies. Absorption spectra of $[\text{CuL}(\text{phen})_2]\text{Cl}$ (**2**) in the absence and presence of DNA are given in Fig. 3.

As the concentration of CT-DNA was increased, the absorption bands of the complexes were affected, resulting in a tendency for hypochromism, and a slight redshift was observed in all of the complexes due to the intercalative binding between DNA and the metal complexes. The “hyperchromic effect” and “hypochromic effect” are spectral features of DNA relating to its double-helix

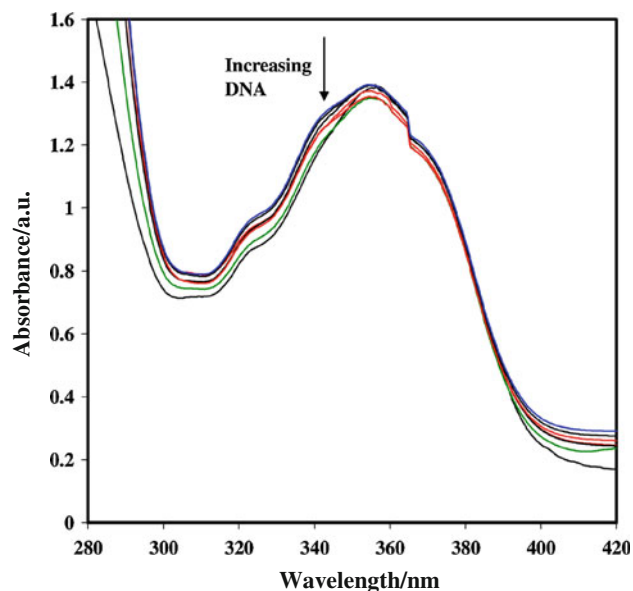


Fig. 3 Absorption spectral changes upon the addition of CT-DNA to a solution of $[\text{CuL}(\text{phen})_2]\text{Cl}$ in buffer (pH 7.2 at 25 °C) and in the presence of increasing amounts of DNA. The arrow indicates the change in absorbance upon increasing the DNA concentration

structure. This spectral change highlighted the changes in the conformation and structure of DNA after complexation with DNA. Hypochromism results from a contraction of the DNA along the axis of the helix, as well as from a change in the conformation of the DNA, while hyperchromism results from damage to the double-helix structure of the DNA [19]. The absorption spectrum of $[\text{CuL}(\text{phen})_2]\text{Cl}$ (**2**) showed an intense absorption band at 354.0 nm, $[\text{CoL}(\text{phen})_2]\text{Cl}$ (**4**) showed such a band at 343 nm, $[\text{NiL}(\text{phen})_2]\text{Cl}$ (**3**) did so at 342.6 nm, and $[\text{ZnL}(\text{phen})_2]\text{Cl}$ (**5**) at 351.9 nm in 5 mM Tris–HCl and 50 mM NaCl buffer solution (pH 7.2). These bands are due to intraligand π – π^* transitions. Increasing the concentration of CT-DNA resulted in a slight bathochromic shift of 2.8–1.9 nm and significant hypochromicity (31–23%). These spectral characteristics clearly suggest that the metal complexes most likely interact with DNA through a mode that involves a stacking interaction between the aromatic chromophore and the base pairs of DNA.

The intrinsic binding constants (K_b) of the metal complexes with CT-DNA were obtained by monitoring the changes in the intraligand band as the concentration of DNA was increased, and applying the following equation:

$$\frac{[\text{DNA}]}{(\varepsilon_a - \varepsilon_f)} = \frac{[\text{DNA}]}{(\varepsilon_b - \varepsilon_f)} + \frac{1}{K_b(\varepsilon_b - \varepsilon_f)},$$

where $[\text{DNA}]$ is the concentration of DNA in base pairs, and the absorption coefficients ε_a , ε_f , and ε_b are the apparent, free, and bound metal complex extinction coefficients, respectively. A plot of $[\text{DNA}]/(\varepsilon_b - \varepsilon_f)$ versus $[\text{DNA}]$ gives a slope of $1/(\varepsilon_b - \varepsilon_f)$ and a Y intercept equal to $[K_b/(\varepsilon_b - \varepsilon_f)]^{-1}$, where K_b is the ratio of the slope to the Y intercept. Intrinsic binding constants of 3.91×10^5 , 2.20×10^5 , 1.78×10^5 , and $1.37 \times 10^5 \text{ M}^{-1}$ were determined for $[\text{CuL}(\text{phen})_2]\text{Cl}$, $[\text{CoL}(\text{phen})_2]\text{Cl}$, $[\text{NiL}(\text{phen})_2]\text{Cl}$, and $[\text{ZnL}(\text{phen})_2]\text{Cl}$, respectively. These values (Table 1) are comparable to that of the classical DNA intercalator ethidium bromide ($1.4 \times 10^6 \text{ M}^{-1}$) [20]. These results suggest that the four metal complexes interact with DNA via an intercalative mode.

Table 1 Electronic absorption spectral properties of Cu(II), Ni(II), Co(II), and Zn(II) complexes

Complex	$\lambda_{\text{max}}/\text{nm}$		$\Delta\lambda/\text{nm}$	$H\%$	$K_b \times 10^5/\text{M}^{-1}$
	Free	Bound			
2	356.8	354.0	2.8	31	3.9
3	342.5	344.8	2.3	28	1.7
4	343.0	345.5	2.5	29	2.2
5	351.5	353.4	1.9	24	1.3

Viscosity measurements

The application of an optical photophysical technique to investigate the interactions of DNA with metal complexes generally provides clues that are needed—but not sufficient by themselves—to support an intercalative binding model. Therefore, viscosity measurements were introduced to provide further support for this type of interaction between the complexes and DNA. In the absence of crystallographic structural data, hydrodynamic methods—which are sensitive to the length of the DNA—are known to be among the definitive and critical indicators of binding strength. Intercalation is an effect of increasing the viscosity of DNA [21]. The significant increase in the viscosity of DNA that occurred upon the addition of a complex was due to intercalation, which caused the DNA bases to separate in order to increase the effective size of the DNA, which could be the reason for the increase in the viscosity. A plot of $(\eta/\eta_0)^{1/3}$ versus $[\text{complex}]/[\text{DNA}]$ (R , Fig. 4) gives a measure of the change in viscosity. A gradual increase in the relative viscosity was observed upon the addition of the metal complexes to the DNA solution, suggesting that the complexes mainly bind via an intercalation mode.

Electrochemical properties of metal complexes

The cyclic voltammogram of $[\text{CuL}(\text{phen})_2]\text{Cl}$ in buffer (pH 7.2 at 25 °C) is given in Fig. 5. The cyclic voltammogram of **2** in the absence of CT-DNA featured three anodic peaks

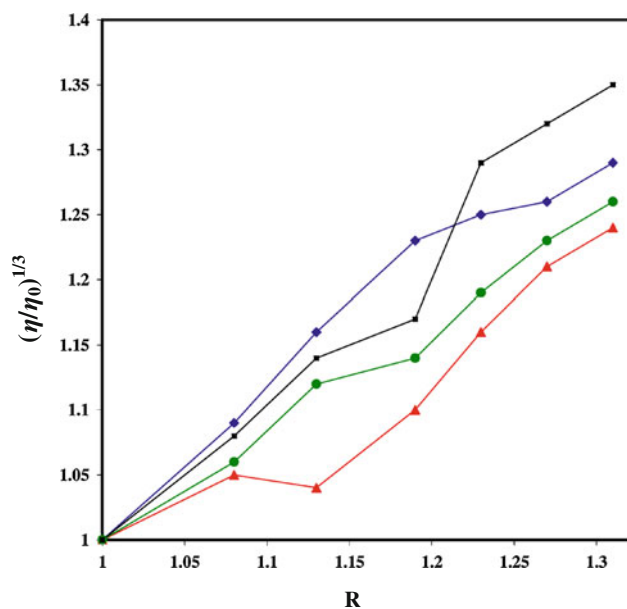


Fig. 4 Effect of increasing amounts of $[\text{CuL}(\text{phen})_2]\text{Cl}$ (filled squares), $[\text{CoL}(\text{phen})_2]\text{Cl}$ (filled diamonds), $[\text{NiL}(\text{phen})_2]\text{Cl}$ (filled circles), and $[\text{ZnL}(\text{phen})_2]\text{Cl}$ (filled triangles) on the viscosity of DNA. $R = [\text{complex}]/[\text{DNA}]$

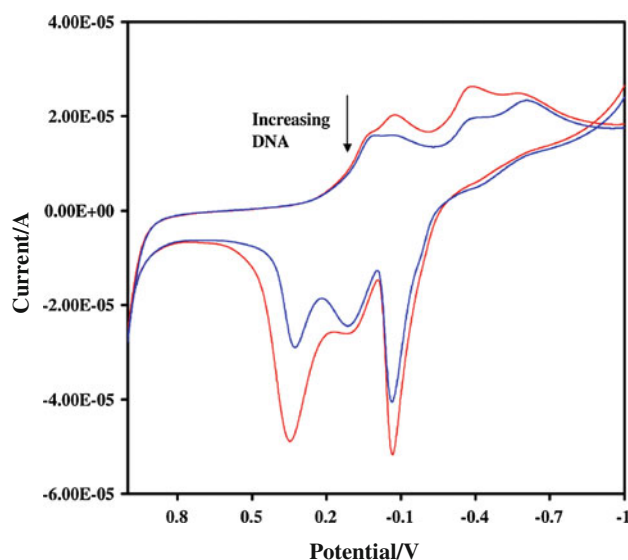


Fig. 5 Cyclic voltammogram of $[\text{CuL}(\text{phen})_2]\text{Cl}$ in the presence of increasing amounts of DNA in buffer (pH 7.2 at 25 °C). The arrow indicates the change in voltammetric currents upon increasing the DNA concentration

($E_{\text{Pa}1} = -0.060$ V, $E_{\text{Pa}2} = -0.097$ V, $E_{\text{Pa}3} = -0.364$ V) and three cathodic peaks ($E_{\text{Pc}1} = -0.617$ V, $E_{\text{Pc}2} = -0.399$ V, $E_{\text{Pc}3} = -0.089$ V). The oxidation of peak $E_{\text{Pa}1}$ refers to $\text{Cu}(0)/\text{Cu}(I)$ and the reduction of $\text{Cu}(I)$ occurred at -0.617 V upon reversing the scan. The anodic and cathodic peak potentials were separated by 0.557 V. The ratio of the anodic to cathodic peak currents, $I_{\text{Pa}}/I_{\text{Pc}} = 1.35$, indicated a quasi-reversible redox process. The oxidation of peak $E_{\text{Pa}2}$ refers to $\text{Cu}(I)/\text{Cu}(II)$ and the reduction of $\text{Cu}(II)$ occurred at -0.399 V upon reversing the scan direction. The anodic and cathodic peak potentials were separated by 0.496 V, and the ratio of the anodic to cathodic peak currents, $I_{\text{Pa}}/I_{\text{Pc}} = 1.40$, indicated a quasi-reversible redox process. The oxidation of peak $E_{\text{Pa}3}$ refers to $\text{Cu}(II)/\text{Cu}(III)$, and the reduction of $\text{Cu}(III)$ occurred at -0.089 V upon reversing the scan direction. The anodic and cathodic peak potentials were separated by 0.453 V, and the ratio of the anodic to cathodic peak currents, $I_{\text{Pa}}/I_{\text{Pc}} = 1.14$, indicated a quasi-reversible redox process. The formal potential $E_{1/2}$, calculated as the average of E_{Pa} and E_{Pc} , was -0.338 , 0.116 , and 0.137 V, respectively. When CT-DNA was added to a solution of the complex, both the anodic and cathodic peak current heights for the complex decreased in the same way with increasing concentrations of DNA (Fig. 5). Also, during DNA addition, the anodic peak potential (E_{Pa}), cathodic peak potential (E_{Pc}), and $E_{1/2}$ (calculated as the average of E_{Pc} and E_{Pa}) all showed positive shifts. These positive shifts are considered to be evidence for intercalation of the complex into the DNA, because this kind of interaction is due to hydrophobic interactions. On the other hand, if a molecule binds

electrostatically to the negatively charged deoxyribose-phosphate backbone of DNA, negative peak potential shifts should be detected. Therefore, the positive shifts in the CV peak potentials of the complex are indicative of an intercalative binding mode of the complex with DNA [22].

The cyclic voltammogram of $[\text{NiL}(\text{phen})_2]\text{Cl}$ in the absence of CT-DNA featured two anodic peaks ($E_{\text{Pa}1} = 0.007 \text{ V}$, $E_{\text{Pa}2} = 0.272 \text{ V}$) and two cathodic peaks ($E_{\text{Pc}1} = 0.411 \text{ V}$, $E_{\text{Pc}2} = -0.178 \text{ V}$). The oxidation of peak $E_{\text{Pa}1}$ refers to Ni(I)/Ni(II), and the reduction of Ni(II) occurred at -0.411 V upon reversing the scan direction. The anodic and cathodic peak potentials were separated by 0.418 V , and the ratio of the anodic to cathodic peak currents, $I_{\text{Pa}}/I_{\text{Pc}} = 1.38$, indicated a quasi-reversible redox process. The oxidation of peak $E_{\text{Pa}2}$ refers to Ni(II)/Ni(III), and reduction of Ni(II) occurred at -0.178 V upon reversing the scan direction. The anodic and cathodic peak potentials were separated by 0.450 V , and the ratio of the anodic to cathodic peak currents, $I_{\text{Pa}}/I_{\text{Pc}} = 1.05$, indicated a quasi-reversible redox process. The formal potentials $E_{1/2}$, taken as the average of E_{Pa} and E_{Pc} , were -0.202 and 0.094 V .

For $\text{Co(III)} \rightarrow \text{Co(II)}$, the redox couple cathodic peak appeared at 0.105 in the absence of CT-DNA ($E_{\text{Pa}} = 0.365 \text{ V}$, $E_{\text{Pc}} = 0.123 \text{ V}$, $\Delta E_{\text{p}} = 0.242 \text{ V}$, and $E_{1/2} = -0.244 \text{ V}$). Note that the ratio $I_{\text{Pa}}/I_{\text{Pc}}$ is approximately unity. This indicates that the reaction of the complex on the glassy carbon electrode surface is a quasi-reversible redox process. The incremental addition of CT-DNA to the complex caused a positive shift in the formal potential ($E_{1/2}$), indicating that $[\text{CoL}(\text{phen})_2]\text{Cl}$ had bonded favorably with DNA via intercalation. Finally, the Zn(II) complex exhibited a quasi-reversible transfer process with the redox couple $\text{Zn(II)} \rightarrow \text{Zn(0)}$, and the cathodic peak appeared at -0.096 V in the absence of DNA ($E_{\text{Pa}} = 0.418 \text{ V}$, $E_{\text{Pc}} = -0.096 \text{ V}$, $\Delta E_{\text{p}} = 0.514 \text{ V}$, and $E_{1/2} = -0.161 \text{ V}$). The ratio of $I_{\text{Pa}}/I_{\text{Pc}}$ is 0.92 , which indicates a quasi-reversible redox process for the metal complex. The incremental addition of CT-DNA to the complex also caused a positive shift in the formal potential ($E_{1/2}$), indicating that $[\text{ZnL}(\text{phen})_2]\text{Cl}$ stabilizes the duplex (GC pairs) by intercalation. The electrochemical parameters of the Cu(II), Ni(II), Co(II), and Zn(II) complexes are shown in Table 2. From these data, it is clear that all of the synthesized complexes interact with DNA via intercalation.

DNA cleavage efficiencies of the metal complexes

Great efforts have been made to develop DNA cleavage compounds due to their potential application in biotechnology and as therapeutic agents. Studies pertaining to DNA cleavage by synthetic reagents are of considerable interest because of their utility as tools in molecular biology. This is true of both sequence-specific DNA cleavers

Table 2 Electrochemical parameters for the interactions of DNA with the Cu(II), Ni(II), Co(II), and Zn(II) complexes

Complex	Redox couple	$E_{1/2}/\text{V}$		$\Delta E_{\text{p}}/\text{V}$		$I_{\text{Pa}}/I_{\text{Pc}}$
		Free	Bound	Free	Bound	
2	$\text{Cu(III)} \rightarrow \text{Cu(II)}$	0.137	0.128	0.453	0.435	1.35
	$\text{Cu(II)} \rightarrow \text{Cu(I)}$	-0.151	-0.116	0.496	0.503	1.40
	$\text{Cu(I)} \rightarrow \text{Cu(0)}$	-0.338	-0.332	0.557	0.554	1.14
3	$\text{Ni(III)} \rightarrow \text{Ni(II)}$	0.094	0.079	0.450	0.469	1.05
	$\text{Ni(II)} \rightarrow \text{Ni(I)}$	-0.202	-0.191	0.418	0.402	1.38
4	$\text{Co(III)} \rightarrow \text{Co(II)}$	0.244	0.260	0.242	0.245	1.18
5	$\text{Zn(II)} \rightarrow \text{Zn(0)}$	0.161	0.178	0.514	0.529	0.92

and DNA footprinting agents. Some chiral complexes have the ability to display enantioselective DNA binding between right- and left-handed DNA. Observations indicate that DNA changes its conformation due to the binding of metal complexes to DNA. DNA cleavage was analyzed by monitoring the conversion of supercoiled DNA (form I) to nicked DNA (form II) and linear DNA (form III) in the presence of the oxidant ascorbic acid.

Figure 6 shows the results of gel electrophoretic separations of plasmid pUC19 DNA induced by the addition of metal(II) complexes in the presence of ascorbic acid. Control experiments using DNA alone did not show any significant cleavage of pUC19 DNA, even with long exposure times (lane 1). Under the same conditions, free ascorbic acid produced no cleavage of pUC19 DNA (lane 2), and the free metal complex alone did not show any apparent cleavage of pUC19 DNA (lane 3). When pUC19 DNA was allowed to interact with metal complexes in the presence of ascorbic acid, the mobility of the band was found to increase slightly, as shown in Fig. 6. These phenomena imply that Cu(II), Co(II), and Ni(II) complexes do more damage to plasmid pUC19 DNA than the Zn(II) complex does in the presence of ascorbic acid.

Antibacterial activity

Multi-drug-resistant Gram-positive and Gram-negative pathogens have become a serious problem in hospitals and the community [23]. To overcome the alarming problem of microbial resistance to antibiotics, the discovery of novel compounds that are active against new targets is a matter of urgency. Hence, nowadays, researchers are focusing their attention to folk medicine, looking for new leads to develop better drugs against bacterial infections. So, at present, pharmaceutical industries are looking for synthesizing the alternative compounds which act as drugs. There is a continuous search for more potent and cheaper raw materials to feed the industry, so pharmaceutical industries are now looking at synthesizing alternative compounds that

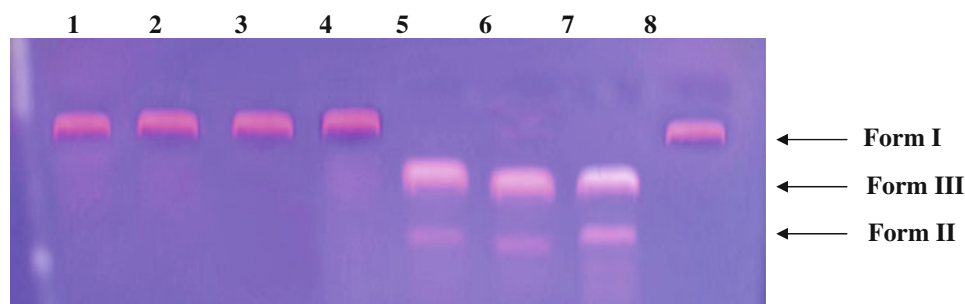


Fig. 6 Changes in the agarose gel electrophoretic pattern of pUC19 DNA induced by ascorbic acid and Cu(II), Ni(II), Co(II), and Zn(II) complexes: lane 1, DNA alone; lane 2, DNA + ascorbic acid; lane 3, DNA + ligand + ascorbic acid; lane 4, DNA + [CuL(phen)₂]Cl;

lane 5, DNA + [CuL(phen)₂]Cl + ascorbic acid; lane 6, DNA + [NiL(phen)₂]Cl + ascorbic acid; lane 7, DNA + [CoL(phen)₂]Cl + ascorbic acid; lane 8, DNA + [ZnL(phen)₂]Cl + ascorbic acid

act as drugs. Much attention is currently focused on the synthesis of new metal complexes and the evaluation of these agents for antibacterial activity. In the present work, we tested the activity of the ligand and its metal(II) complexes against bacteria. Ampicillin was used as a standard drug for comparison. The microorganisms used in the present investigations included *Staphylococcus aureus* and *Bacillus subtilis* (Gram-positive bacteria) and *Pseudomonas aeruginosa*, *Escherichia coli*, and *Salmonella typhi* (Gram-negative bacteria). The diffusion agar technique was used to evaluate the antibacterial activities of the synthesized mixed-ligand complexes. Biocidal activity data for the investigated compounds are summarized in Table 3.

From this table, we can infer that all of the metal complexes have greater inhibitory effects than the free ligand. The higher antimicrobial activities of the metal complexes compared to the Schiff base may be due to changes in structure that occur due to coordination and chelation that cause the metal complexes to act as more powerful antibacterial agents.

Chelation reduces the polarity of the metal ion considerably because of the partial sharing of its positive charge with donor groups, and also due to π -electron delocalization across the whole chelating ring. Lipids and polysaccharides are important constituents of the cell wall and membranes that are preferred for metal ion interactions. The cell wall

Table 3 Minimum inhibitory concentrations (in mg cm⁻³) of the synthesized compounds with respect to the growth of five bacteria species

Compound	<i>S. aureus</i>	<i>P. aeruginosa</i>	<i>E. coli</i>	<i>B. subtilis</i>	<i>S. typhi</i>
1	8	11	6	10	13
2	19	23	25	27	31
3	15	18	21	19	24
4	17	21	18	21	19
5	17	14	20	23	21
Ampicillin	12	16	14	16	19

also contains many phosphates, carbonyls, and cysteinyl ligands that maintain the integrity of the membrane by acting as a barrier to diffusion and also provide suitable sites for binding. Furthermore, increased lipophilicity enhances the penetration of the complexes into the lipid membrane and the blocking of metal-binding sites in the enzymes of microorganisms [24]. While chelation is not the only criterion for antibacterial activity, it is an intricate blend of several factors such as the nature of the metal ion and the ligand, the geometry of the metal complex, the lipophilicity, the presence of co-ligands, and steric and pharmacokinetic factors.

Conclusion

Four mixed-ligand Cu(II), Ni(II), Co(II), and Zn(II) complexes of the tryptophan-containing Schiff base **1** and 1,10-phenanthroline have been synthesized and characterized. Elemental, conductivity, and FAB-MS analyses revealed the stoichiometry and composition of the complexes of [ML(phen)₂]Cl. FT-IR, UV-Vis, ¹H NMR, and EPR spectral data, as well as magnetic measurements, confirmed the bonding features of the above mixed-ligand complexes. The binding of these complexes to CT-DNA was investigated in detail via electronic absorbance titration, viscosity, and cyclic voltammetry. The experimental results reveal that all of the complexes can interact with DNA through an intercalative binding mode. The results of agarose gel electrophoresis indicate that the complexes exhibit the ability to cleave pUC19 DNA in the presence of ascorbic acid. A study of the antibacterial activities of the complexes showed that they all exhibit good biological activity against different organisms.

Experimental

All reagents, tryptophan, benzaldehyde, and metal(II) chlorides were Merck products and used as supplied.

Commercial solvents were distilled and then used to prepare the ligand and its complexes. DNA was purchased from Bangalore Genei (India). Microanalyses (C, H, N) were performed on a Carlo Erba 1108 analyzer at the Sophisticated Analytical Instrument Facility (SAIF), Central Drug Research Institute (CDRI), Lucknow, India. Molar conductivities were measured via 10^{-3} mol/dm³ solutions in DMSO at room temperature using a Systronic model 304 digital conductivity meter. Magnetic susceptibility measurements of the complexes were carried out using a Gouy balance with copper sulfate pentahydrate employed as the calibrant. IR spectra were recorded with a Shimadzu spectrophotometer in the 4,000–400 cm⁻¹ range using KBr pellets. NMR spectra were recorded on a Bruker Avance 300 FT-NMR spectrometer in CDCl₃ using TMS as the internal reference. FAB-MS spectra were recorded with a VGZAB-HS spectrometer at room temperature in a 3-nitrobenzylalcohol matrix. EPR spectra were recorded on a Varian E 112 EPR spectrometer in DMSO solution at both room temperature (300 K) and LNT (77 K) using diphenylpicrylhydrazyl as the *g*-marker. The absorption spectra were recorded using a Shimadzu model UV-1601 spectrophotometer at room temperature.

Potassium 2-(benzylideneamino)-3-(indol-3-yl)propionate (**1**, C₁₈H₁₅KN₂O₂)

Tryptophan (2.04 g, 0.01 mol) was dissolved in 40 cm³ of a water–ethanol mixture (1:1) and added to a hot ethanolic solution (30 cm³) of KOH. The resulting solution was stirred to obtain a homogeneous solution. Then, an ethanolic solution of 1.06 g benzaldehyde (0.01 mol) was added to this solution dropwise, and the resultant mixture was refluxed for ca. 5 h. A pale yellow colored solution was obtained, which was reduced to one-third on a water bath. The solid complex that precipitated was filtered off, washed thoroughly with ethanol, and dried in vacuo. Yield 77%; FT-IR (KBr): $\bar{\nu} = 3,252$ (NH), 1,581 (HC=N), 1,456 $\nu_{\text{asy}}(\text{COO})$, 1,375 $\nu_{\text{sy}}(\text{COO})$ cm⁻¹; ¹H NMR (CDCl₃): $\delta = 10.30$ (s, 1H, NH), 8.90 (s, 1H, CH=N), 7.49–7.77 (m, 5H, phenyl), 6.81–7.39 (m, 5H, indole), 2.70 (q, 1H, CH), 2.40 (t, 2H, CH₂) ppm; ¹³C NMR (CDCl₃): $\delta = 53.90$ (CH₂), 55.40 (CH), 105.62, 108.15, 111.82, 112.37, 117.95 (aromatic C), 118.74, 121.40, 125.11, 126.33, 128.53, 136.62 (indole C), 167.11 (CH=N), 171.56 (COO⁻) ppm; UV-Vis (DMSO): $\lambda_{\text{max}} = 42,564, 36,978$ cm⁻¹; MS: *m/z* = 330.

Synthesis of [ML(phen)₂]Cl complexes

The complexes were prepared by mixing the appropriate molar quantity of the ligand **1** with the metal salt using the following procedure: an ethanolic solution of **1** (0.003 mol) was stirred with 5 cm³ of an ethanolic solution of the

anhydrous metal(II) chloride (0.003 mol) for ca. 1 h. A methanolic solution (5 cm³) of 1,10-phenanthroline (0.006 mol) was added to this mixture, and the stirring was continued for 1 h. The solid product obtained was filtered and washed with ethanol.

2-(Benzylideneamino)-3-(indol-3-yl)propionatebis-(1,10-phenanthroline)copper(II) chloride

(**2**, C₄₂H₃₁ClCuN₆O₂)

Yield 86%; FT-IR (KBr): $\bar{\nu} = 3,252$ (NH), 1,581 (HC=N), 1,427 $\nu_{\text{asy}}(\text{COO})$, 1,315 $\nu_{\text{sy}}(\text{COO})$, 511 (M=O), 478 (M=N) cm⁻¹; $\Lambda_m = 45.37 \Omega^{-1} \text{cm}^2 \text{mol}^{-1}$; $\mu_{\text{eff}} = 1.76$ BM; UV-Vis (DMSO): $\lambda_{\text{max}} = 31,496, 27,248, 13,586$ cm⁻¹; MS: *m/z* = 715.

2-(Benzylideneamino)-3-(indol-3-yl)propionatebis-(1,10-phenanthroline)nickel(II) chloride

(**3**, C₄₂H₃₁ClNiN₆O₂)

Yield 76%; FT-IR (KBr): $\bar{\nu} = 3,252$ (NH), 1,571 (HC=N), 1,431 $\nu_{\text{asy}}(\text{COO})$, 1,315 $\nu_{\text{sy}}(\text{COO})$, 516 (M=O), 473 (M=N) cm⁻¹; $\Lambda_m = 51.23 \Omega^{-1} \text{cm}^2 \text{mol}^{-1}$; $\mu_{\text{eff}} = 3.21$ BM; UV-Vis (DMSO): $\lambda_{\text{max}} = 23,392, 17,168, 14,749$ cm⁻¹; MS: *m/z* = 710.

2-(Benzylideneamino)-3-(indol-3-yl)propionatebis-(1,10-phenanthroline)cobalt(II) chloride

(**4**, C₄₂H₃₁ClCoN₆O₂)

Yield 71%; FT-IR (KBr): $\bar{\nu} = 3,256$ (NH), 1,593 (HC=N), 1,436 $\nu_{\text{asy}}(\text{COO})$, 1,317 $\nu_{\text{sy}}(\text{COO})$, 507 (M=O), 481 (M=N) cm⁻¹; $\Lambda_m = 55.40 \Omega^{-1} \text{cm}^2 \text{mol}^{-1}$; $\mu_{\text{eff}} = 4.88$ BM; UV-Vis (DMSO): $\lambda_{\text{max}} = 22,652, 17,513, 14,992$ cm⁻¹; MS: *m/z* = 710.

2-(Benzylideneamino)-3-(indol-3-yl)propionatebis-(1,10-phenanthroline)zinc(II) chloride

(**5**, C₄₂H₃₁ClZnN₆O₂)

Yield 73%; FT-IR (KBr): $\bar{\nu} = 3,256$ (NH), 1,604 (HC=N), 1,444 $\nu_{\text{asy}}(\text{COO})$, 1,319 $\nu_{\text{sy}}(\text{COO})$, 503 (M=O), 478 (M=N) cm⁻¹; ¹H NMR (CDCl₃): $\delta = 10.61$ (s, 1H, NH), 8.60 (s, 1H, CH=N), 7.77–8.26 (m, 16H, phen), 7.01–7.43 (m, 5H, phenyl), 6.63–6.94 (m, 5H, indole), 3.20 (q, 1H, CH), 2.60 (t, 2H, CH₂) ppm; ¹³C NMR (CDCl₃): $\delta = 52.60$ (CH), 54.02 (CH₂), 105.43, 108.15, 113.79, 112.85, 118.45 (aromatic C), 120.25, 125.97, 127.57, 129.18, 139.94, 147.54 (indole C), 157.25 (CH=N), 165.47 (COO⁻) ppm; $A_m = 58.75 \Omega^{-1} \text{cm}^2 \text{mol}^{-1}$; UV-Vis (DMSO): $\lambda_{\text{max}} = 33,112, 29,492$ cm⁻¹; MS: *m/z* = 717.

DNA-binding experiments

The interactions between the metal complexes and DNA were studied using electronic absorption spectroscopic, viscosity, and electrochemical methods. Disodium salt of calf thymus DNA was stored at 4 °C. A solution of DNA in the buffer 50 mM NaCl, 5 mM Tris HCl (pH 7.2) in water

gave a UV absorbance ratio at 260 and 280 nm, A_{260}/A_{280} , of 1.9:1, indicating that the DNA was sufficiently free from protein [25]. The concentration of DNA was measured using its extinction coefficient at 260 nm ($6,600 \text{ M}^{-1}$) after 1:100 dilution. Stock solutions were stored at 4°C and used for no more than 4 days. Doubly distilled water was used to prepare solutions. Concentrated stock solutions of the complexes were prepared by dissolving the complexes in DMF and diluting suitably with the corresponding buffer to the required concentration in all experiments. Absorption titration experiments were carried out by varying the DNA concentration and keeping the complex concentration constant. Absorbance values were recorded after each successive addition of DNA solution and equilibration (ca. 10 min). The absorption data were analyzed to evaluate the intrinsic binding constant K_b using the reported procedure [26].

Electrochemical studies were carried out using a CHI electrochemical analyzer controlled by CHI620C software. CV measurements were performed using a glassy carbon working electrode and an Ag/AgCl reference electrode, and the supporting electrolyte was 50 mM NaCl, 5 mM Tris buffer (pH 7.2). All solutions were deoxygenated by purging with N_2 for 30 min prior to measurements.

Viscosity measurements at room temperature were carried out using a semi-micro dilution capillary viscometer. Each experiment was performed three times, and an average flow time was calculated. Data are presented as (η/η_0) versus the binding ratio, where η is the viscosity of DNA in the presence of the complex and η_0 is the viscosity of DNA alone.

Methodology used for the pUC19 DNA cleavage study

The cleavage of pUC19 DNA was determined by agarose gel electrophoresis. The gel electrophoresis experiments were performed by incubating samples containing 10 mmol/dm^3 pUC19 DNA, 30 mmol/dm^3 of the metal complex, and 10 mmol/dm^3 ascorbic acid in Tris-HCl/NaCl buffer (pH 7.2) at 37°C for 2 h. After incubation, the samples were electrophoresed for 2 h at 50 V on 1% agarose gel using Tris-acetic acid-EDTA buffer (pH 7.2). The gel was then stained using $1 \mu\text{g/cm}^3$ ethidium bromide and photographed under ultraviolet light at 360 nm. All of the experiments were performed at room temperature unless otherwise stated.

Methodology used for antibacterial analysis

The in vitro antibacterial activities of the ligand and its complexes were tested against the bacteria *S. aureus*,

B. subtilis, *P. aeruginosa*, *E. coli*, and *S. typhi* by the paper disc method using nutrient agar as the medium. The solution was prepared by dissolving the compound in DMSO, and the entire blank discs were moistened with the solvent. To perform disc assays, paper (6 mm) containing the compound was placed on nutrient agar plates onto which 0.1 cm^3 of overnight cultures of microorganisms had already been spread. The diameter of the inhibition zone was measured after 36 h of incubation at 37°C .

Acknowledgments The authors express their sincere thanks to the College Managing Board, the Principal, and the Head of the Department of Chemistry, VHNSN College, Virudhunagar, India for providing the necessary research facilities. NR thanks the University Grants Commission (UGC), New Delhi for financial assistance.

References

- Jain S, Longia S, Ramnani VK (2009) People's J Sci Res 2:37
- Berthon G, Blais MJ, Piktas M, Houghbossa K (1984) J Inorg Biochem 20:113
- Kiss T, Gergely A (1985) J Inorg Biochem 25:247
- Hinojosa M, Ortiz R, Perello L, Borrás J (1987) J Inorg Biochem 29:119
- Manjul V, Chakraborty D, Bhattacharya PK (1990) Indian J Chem A 29:577
- Chakraborty D, Bhattacharya PK (1990) J Inorg Biochem 39:1
- Padmavathi M, Satyanarayana S (1997) Indian J Chem A 36:1001
- Ceakor S, Biceer E, Ceakor O (2000) Electrochem Commun 2:124
- Lau S, Sarkar B (1975) Can J Chem 53:710
- Shahabadi N, Kashanian S, Darabi F (2010) Eur J Med Chem 45:4239
- Xiong Y, Ji LN (1999) Coord Chem Rev 185:711
- Sigman DS, Mazumder A, Perrin DM (1993) Chem Rev 93:2295
- Boon EM, Barton JK, Pradeepkumar PI, Isaksson J, Petit C, Chattopadhyaya J (2002) Angew Chem Int Ed 41:3402
- Metcalfe C, Thomas JA (2003) Chem Soc Rev 32:215
- Sathiyaraj G, Weyhermuller T, Unni Nair B (2010) Eur J Med Chem 45:284
- Kaur S, Modi NH, Panda D, Roy N (2010) Eur J Med Chem 45:4209
- Raman N, Sobha S, Thamaraiichelvan A (2011) Spectrochim Acta Part A 78:888
- Raman N, Thalamuthu S, Dhaweethuraja J, Neelakandan MA, Banerjee S (2008) J Chil Chem Soc 53:1439
- Colak A, Terzi U, Col M, Karaoglu SA, Karabocek S, Kucukdumlu A, Ayaz FA (2010) Eur J Med Chem 45:5169
- Lepecp JB, Paoletti C (1967) J Mol Biol 27:87
- Satyanarayana S, Dabrowiak JC, Chaires JB (1993) Biochemistry 32:2573
- Ni Y, Lin D, Kokat S (2006) Anal Biochem 352:23
- Cheng K, Zheng Q-Z, Hou J, Zhou Y, Liu C-H, Zhao J, Zhu H-L (2010) Bioorg Med Chem 18:2447
- Ramesh R, Maheswaran S (2003) J Inorg Biochem 96:457
- Marmur J (1961) J Mol Biol 3:208
- Wolfe A, Shimer GH, Meehan T (1987) Biochemistry 26:6392